

Fast Embedding for JOFC Using the Raw Stress Criterion

Vince Lyzinski¹, Youngser Park², Carey E. Priebe³, Michael Trosset⁴

¹Johns Hopkins University Human Language Technology Center of Excellence, Baltimore, MD, USA

²Center for Imaging Sciences, Johns Hopkins University, Baltimore, MD, USA

³Department of Applied Mathematics and Statistics, Johns Hopkins University, Baltimore, MD, USA

⁴Department of Statistics, Indiana University, Bloomington, IN, USA

Tuesday 3rd December, 2024

Abstract

The Joint Optimization of Fidelity and Commensurability (JOFC) manifold matching methodology embeds an omnibus dissimilarity matrix consisting of multiple dissimilarities on the same set of objects. One approach to this embedding optimizes the preservation of fidelity to each individual dissimilarity matrix together with commensurability of each given observation across modalities via iterative majorizations of a raw stress error criterion by successive Guttman transforms. In this paper, we exploit the special structure inherent to JOFC to exactly and efficiently compute the successive Guttman transforms, and as a result we are able to greatly speed up and parallelize the JOFC procedure. We demonstrate the scalability of our implementation on both real and simulated data examples.

1 Introduction

Consider n objects, each measured under m disparate modalities or conditions, each modality yielding an object-wise dissimilarity matrix $\Delta_1, \Delta_2, \dots, \Delta_m \in \mathbb{R}^{n \times n}$. The Joint Optimization of Fidelity and Commensurability (JOFC) algorithm [21] simultaneously embeds these mn data points (n objects in m modalities) into a common Euclidean space by embedding an omnibus dissimilarity matrix Δ which encapsulates the information contained in the dissimilarities $\{\Delta_i\}_{i=1}^m$. One approach to this embedding optimizes the preservation of fidelity to each individual dissimilarity matrix (i.e., preserving the within modality dissimilarities) together with commensurability of each given observation across modalities (i.e., preserving the cross-modality matchedness of the

data). This approach embeds Δ by minimizing Kruskal’s raw stress criterion for metric multidimensional scaling via successive Guttman transforms [2] (see Algorithm 1).

In this paper, we exploit the special structure of the JOFC weight matrix to exactly and efficiently compute these successive Guttman transforms. Employing this and further computational simplifications, we are able to dramatically speed up and parallelize the JOFC procedure (see Algorithm 2). Lastly, in Section 3 we demonstrate these speed-ups on real and synthetic data examples.

1.1 Background

Manifold matching—embedding multiple modality data sets into a common low-dimensional space wherein joint inference can be investigated—is an important inference task in statistical pattern recognition, with applications in computer vision (see, for example, [19, 11, 8, 29]), text and language processing (see, for example, [14, 26, 22]), and machine learning (see, for example, [27, 28, 16]), to name a few; for a survey of the literature on manifold matching and the broader problem of transfer learning, see [20]. JOFC has proven to be an effective and flexible manifold matching procedure, with numerous applications and extensions in the literature [18, 24, 17, 1, 23].

2 The JOFC algorithm

Assuming that the entire cross-modality correspondence is known *a priori* between the n objects, the JOFC we consider proceeds by embedding the omnibus dissimilarity matrix

$$\Delta = [\Delta_{i,j}] = \begin{bmatrix} \Delta_1 & \eta & \eta & \cdots & \eta \\ \eta & \Delta_2 & \eta & \cdots & \eta \\ \eta & \eta & \Delta_3 & & \eta \\ \vdots & \vdots & \vdots & \ddots & \vdots \\ \eta & \eta & \eta \cdots & \cdots & \Delta_m \end{bmatrix} \in \mathbb{R}^{mn \times mn}$$

via the SMACOF algorithm [3] for raw stress multidimensional scaling. Here,

$$\eta = \begin{bmatrix} 0 & \text{NA} & \cdots & \text{NA} \\ \text{NA} & 0 & \cdots & \text{NA} \\ \vdots & \vdots & \ddots & \vdots \\ \text{NA} & \text{NA} & \cdots & 0 \end{bmatrix} \in \mathbb{R}^{n \times n}$$

represents the assumption that the inter-object, cross-modality dissimilarities are *not* available, and so are treated as missing data (NA representing “Not Available”) in the embedding procedure.

In this missing data setting, the associated weight matrix used in the embedding is (where $J_n = \mathbf{1}_n \mathbf{1}_n^T \in \mathbb{R}^{n \times n}$ and $\mathbf{1}_n$ is the column vector of all one’s in \mathbb{R}^n) given by

$$\mathbf{W} = [W_{i,j}] = \begin{bmatrix} J_n - I_n & wI_n & wI_n & \cdots & wI_n \\ wI_n & J_n - I_n & wI_n & \cdots & wI_n \\ wI_n & wI_n & J_n - I_n & \cdots & wI_n \\ \vdots & \vdots & \vdots & \ddots & \vdots \\ wI_n & wI_n & wI_n \cdots & \cdots & J_n - I_n \end{bmatrix} \in \mathbb{R}^{mn \times mn}.$$

Note that the parameter w appearing above allows us to weight the commensurability versus the fidelity of the embedding (see Eq. (1) for detail).

Remark 1. In [21], the missing cross-modality dissimilarity between modality i and modality j was imputed as $(\Delta_i + \Delta_j)/2$, and $\mathbf{\Delta}$ was embedded using classical multidimensional scaling. Here we choose not to impute the missing data for two main reasons: imputing the cross-modality dissimilarities potentially increases the variance in our embedded points; and the special structure of \mathbf{W} in the missing data setting allows us to greatly speed up and parallelize the JOFC procedure (see Section 2.1). In addition, in many real data settings (see Section 3.2) the n objects originate from *disparate* data sources and are not simply repeated measurements of the same objects in a single space, which further complicates the very concept of cross-modality dissimilarities.

For $i = 1, 2, \dots, m$, let $X_1^{(i)}, X_2^{(i)}, \dots, X_n^{(i)}$ be the embedded points in \mathbb{R}^d corresponding to Δ_i . Writing

$$\mathbf{X}^\top = [(\mathbf{X}^{(1)})^\top | (\mathbf{X}^{(2)})^\top | \dots | (\mathbf{X}^{(m)})^\top] \in \mathbb{R}^{mn \times d},$$

where for $i = 1, 2, \dots, m$,

$$(\mathbf{X}^{(i)})^\top = [(X_1^{(i)})^\top | (X_2^{(i)})^\top | \dots | (X_n^{(i)})^\top] \in \mathbb{R}^{n \times d},$$

the JOFC routine attempts to find a configuration $\mathbf{X} \in \mathbb{R}^{mn \times d}$ of mn points that minimizes the raw stress error criterion

$$\sigma(\mathbf{X}) = \sum_{i < j} W_{i,j} (\Delta_{i,j} - d_{i,j}(\mathbf{X}))^2,$$

where $d_{i,j}(\mathbf{X})$ is the Euclidean distance between the i th and j th rows of \mathbf{X} . Note that the form of

\mathbf{W} allows us to write $\sigma(\mathbf{X})$ in a form more amenable to fast computation,

$$\sigma(\mathbf{X}) = \underbrace{\sum_{i=1}^m \sum_{1 \leq j < \ell \leq n} ([\Delta_i]_{j,\ell} - d_{j,\ell}(\mathbf{X}^{(i)}))^2}_{\text{fidelity}} + w \underbrace{\sum_{1 \leq i < j \leq m} \sum_{\ell=1}^n d(X_\ell^{(i)}, X_\ell^{(j)})^2}_{\text{commensurability}}, \quad (1)$$

where $d(\cdot, \cdot)$ is the Euclidean distance function.

Remark 2. Note that Eq. (1) emphasizes the role of w in weighting the fidelity versus the commensurability of the embedding. If $w \ll 1$, then the optimal embedding will preserve the within-modality dissimilarities at the expense of the cross-modality correspondence. If $w \gg 1$, then the optimal embedding will preserve the cross-modality correspondence at the expense of the within-modality dissimilarities. Choosing an optimal w is the subject of active research, see [1] for detail. We also note that setting $w = 0$ would be equivalent to separately embedding the Δ'_i s via raw stress MDS, which would optimize fidelity without regard for commensurability. At the other extreme, setting $w = \infty$ would be akin to CCA (canonical correlation analysis), which optimizes embedding commensurability without regard for fidelity.

Remark 3. From Eq. (1), we see that to compute $\sigma(\mathbf{X})$, we do not need to compute all $\binom{mn}{2}$ pairwise distance between rows of \mathbf{X} , as we only need to compute $m\binom{n}{2} + \binom{m}{2}n$ interpoint distances. Furthermore, the fidelity can be written as

$$\sum_{i=1}^m \sum_{1 \leq j < \ell \leq n} ([\Delta_i]_{j,\ell} - d_{j,\ell}(\mathbf{X}^{(i)}))^2 = \frac{1}{2} \sum_{i=1}^m \|\Delta_i - d(\mathbf{X}^{(i)})\|_F^2,$$

and each of the $\|\Delta_i - d(\mathbf{X}^{(i)})\|_F^2$ can be computed in parallel. The commensurability requires $\binom{m}{2}$ paired distance calculations amongst the n points across the m modalities, each of which can be computed in parallel.

Letting \mathbf{L} be the combinatorial Laplacian of the weight matrix \mathbf{W} and defining

$$B(\mathbf{X})_{i,j} := \begin{cases} \frac{-W_{i,j}\Delta_{i,j}}{d_{i,j}(\mathbf{X})} & \text{if } i \neq j \text{ and } d_{i,j}(\mathbf{X}) \neq 0 \\ 0 & \text{if } i \neq j \text{ and } d_{i,j}(\mathbf{X}) = 0 \\ -\sum_{k=1, k \neq i}^n B(\mathbf{X})_{i,k} & \text{if } i = j, \end{cases}$$

the stationary equation $\nabla\sigma(\mathbf{X}) = 0$ can be written as $\mathbf{L}\mathbf{X} = B(\mathbf{X})\mathbf{X}$. The Guttman transform updates a configuration $\mathbf{X}_{(i-1)}$ by solving $\mathbf{L}\mathbf{X} = B(\mathbf{X}_{(i-1)})\mathbf{X}_{(i-1)}$; in the multidimensional scaling literature, this transformation is often written as $\mathbf{X}_{(i)} = \Gamma(\mathbf{X}_{(i-1)}) = \mathbf{L}^\dagger B(\mathbf{X}_{(i-1)})\mathbf{X}_{(i-1)}$. Notice

Algorithm 1 JOFC Algorithm for Manifold Matching (see Section 2 for detail)

Require: Omnibus dissimilarity matrix Δ , weight matrix \mathbf{W} , embedding dimension d , $\text{tol} = \epsilon$

Ensure: $\mathbf{X} \in \mathbb{R}^{mn \times d}$, a configuration of points in \mathbb{R}^d

- 1: Choose an initialization $\mathbf{X}_{(0)}$ via cMDS (classical MDS, see [25, 2]) of Δ
 - 2: Compute $\sigma(\mathbf{X}_{(0)})$
 - 3: **while** $\sigma(\mathbf{X}_{(i)}) - \sigma(\mathbf{X}_{(i-1)}) > \epsilon$ **do**
 - 4: $\mathbf{X}_{(i)} = \mathbf{L}^\dagger B(\mathbf{X}_{(i-1)}) \mathbf{X}_{(i-1)}$
 - 5: Compute $\sigma(\mathbf{X}_{(i)})$
 - 6: **end while**
 - 7: Output the final iteration $\mathbf{X}_{(\text{final})}$
-

that $\mathbf{X}_{(i)}$ is centered at zero if $\mathbf{X}_{(i-1)}$ is centered at zero. For JOFC, the resulting iterative algorithm is summarized in Algorithm 1. The sequence of steps generated by successive Guttman transforms can also be derived via majorization; hence, Algorithm 1 is closely related to the popular SMACOF algorithm for metric multidimensional scaling [5, 4].

In general, \mathbf{L}^\dagger must be calculated by singular value or QR decomposition, which may be prohibitively expensive if mn is large, with computational complexity of order $O(m^3n^3)$. Fortunately, there are many applications in which the special structure of the weight matrix \mathbf{W} allows for direct calculation of \mathbf{L}^\dagger , sometimes with subsequent simplification of $\mathbf{L}^\dagger B(\mathbf{X}_{(i-1)}) \mathbf{X}_{(i-1)}$. Examples include the familiar case of unit weights and the case of symmetric block-circulant matrices [10, 9]. In Section 2.1, we demonstrate that the special structure of JOFC also permits the direct calculation of \mathbf{L}^\dagger which then results in a much simplified calculation of $\mathbf{L}^\dagger B(\mathbf{X}_{(i-1)}) \mathbf{X}_{(i-1)}$.

2.1 Fast JOFC

We next provide the necessary details for our fast implementation of Algorithm 1, which we present in Algorithm 2. First, we demonstrate that the form of our weight matrix \mathbf{W} allows us to algebraically compute \mathbf{L}^\dagger .

Proposition 4. *With notation as above,*

$$\mathbf{L}^\dagger = \left(\mathbf{L} + \frac{1}{mn} J_{mn} \right)^{-1} - \frac{1}{mn} J_{mn} = \begin{bmatrix} A & C & C & \cdots & C \\ C & A & C & \cdots & C \\ C & C & A & \cdots & C \\ \vdots & \vdots & \vdots & \ddots & \vdots \\ C & C & C & \cdots & A \end{bmatrix} \in \mathbb{R}^{mn \times mn}, \quad (2)$$

where

$$A = \frac{n+w}{n(n+mw)} I_n + \left(\frac{-m^2w^2 + mn^2 - mnw - n^2}{wn^2m^2(n+wm)} \right) J_n \in \mathbb{R}^{n \times n},$$

and

$$C = \frac{w}{n(n+mw)} I_n + \left(\frac{-m^2w^2 - mnw - n^2}{wn^2m^2(n+wm)} \right) J_n \in \mathbb{R}^{n \times n}.$$

Proof. We first note that $J_{mn}\mathbf{L} = \mathbf{L}J_{mn} = 0$, so that

$$\left(\mathbf{L} + \frac{1}{mn} J_{mn} \right) J_{mn} = J_{mn} = J_{mn} \left(\mathbf{L} + \frac{1}{mn} J_{mn} \right).$$

We then calculate

$$\begin{aligned} \mathbf{L} \left[\left(\mathbf{L} + \frac{1}{mn} J_{mn} \right)^{-1} - \frac{1}{mn} J_{mn} \right] \mathbf{L} &= \mathbf{L} \left(\mathbf{L} + \frac{1}{mn} J_{mn} \right)^{-1} \mathbf{L} \\ &= \mathbf{L} \left(\mathbf{L} + \frac{1}{mn} J_{mn} \right)^{-1} \left(\mathbf{L} + \frac{1}{mn} J_{mn} - \frac{1}{mn} J_{mn} \right) \\ &= \mathbf{L} \left(I_{mn} - \frac{1}{mn} J_{mn} \right) = \mathbf{L}; \end{aligned}$$

and

$$\begin{aligned} &\left[\left(\mathbf{L} + \frac{1}{mn} J_{mn} \right)^{-1} - \frac{1}{mn} J_{mn} \right] \mathbf{L} \left[\left(\mathbf{L} + \frac{1}{mn} J_{mn} \right)^{-1} - \frac{1}{mn} J_{mn} \right] \\ &= \left[\left(\mathbf{L} + \frac{1}{mn} J_{mn} \right)^{-1} - \frac{1}{mn} J_{mn} \right] \left(\mathbf{L} + \frac{1}{mn} J_{mn} - \frac{1}{mn} J_{mn} \right) \left[\left(\mathbf{L} + \frac{1}{mn} J_{mn} \right)^{-1} - \frac{1}{mn} J_{mn} \right] \\ &= \left[I_{mn} - 2\frac{1}{mn} J_{mn} + J_{mn} \right] \left[\left(\mathbf{L} + \frac{1}{mn} J_{mn} \right)^{-1} - \frac{1}{mn} J_{mn} \right] = \left(\mathbf{L} + \frac{1}{mn} J_{mn} \right)^{-1} - \frac{1}{mn} J_{mn}; \end{aligned}$$

and $\left[\left(\mathbf{L} + \frac{1}{mn} J_{mn} \right)^{-1} - \frac{1}{mn} J_{mn} \right] \mathbf{L} = I_{mn} - \frac{1}{mn} J_{mn} = \mathbf{L} \left[\left(\mathbf{L} + \frac{1}{mn} J_{mn} \right)^{-1} - \frac{1}{mn} J_{mn} \right] \mathbf{L}$ is Hermitian.

It follows that

$$\mathbf{L}^\dagger = \left(\mathbf{L} + \frac{1}{mn} J_{mn} \right)^{-1} - \frac{1}{mn} J_{mn}.$$

It is straightforward (though tedious) to verify that \mathbf{L}^\dagger has the block-matrix form specified in (2); details are suppressed here and are spelled out fully in Appendix A. \square

Remark 5. Even given identical initializations, the fJOFC algorithm (Algorithm 2), and the JOFC algorithm may not give identical embeddings of $\mathbf{\Delta}$, as JOFC relies on a computational approximation of \mathbf{L}^\dagger , while fJOFC exactly algebraically computes \mathbf{L}^\dagger .

Algorithm 2 fJOFC: Fast JOFC Algorithm for Manifold Matching

Require: Omnibus dissimilarity matrix Δ , weight matrix \mathbf{W} , embedding dimension d , $\text{tol} = \epsilon$

Ensure: $\mathbf{X} \in \mathbb{R}^{mn \times d}$, a configuration of points in \mathbb{R}^d

- 1: Set ξ_0 to be the configuration obtained via cMDS of $(\sum_i \Delta_i) / m$
 - 2: **parfor** $i=1, 2, \dots, m$ **do**
 - 3: Set ξ_i to be the configuration obtained via cMDS of Δ_i
 - 4: Set $\mathbf{X}_{(0)}^{(i)}$ to be the orthogonal Procrustes fit (with translation) of ξ_i onto ξ_0
 - 5: **end parfor**
 - 6: Set $\mathbf{X}_{(0)}^\top = \left[(\mathbf{X}_{(0)}^{(1)})^\top \mid (\mathbf{X}_{(0)}^{(2)})^\top \mid \dots \mid (\mathbf{X}_{(0)}^{(m)})^\top \right]$
 - 7: Compute $\sigma(\mathbf{X}_{(0)})$ as in Remark 3
 - 8: **while** $\sigma(\mathbf{X}_{(i)}) - \sigma(\mathbf{X}_{(i-1)}) > \epsilon$ **do**
 - 9: **parfor** $j=1, 2, \dots, m$ **do**
 - 10: Compute $B(\mathbf{X}_{(i-1)}^{(j)})$
 - 11: Set $x_j = B(\mathbf{X}_{(i-1)}^{(j)})\mathbf{X}_{(i-1)}^{(j)}$
 - 12: **end parfor**
 - 13: **parfor** $j=1, 2, \dots, m$ **do**
 - 14: Set $\mathbf{X}_{(i)}^{(j)} = \frac{n+w}{n(n+nw)}x_j + \sum_{\ell \neq j} \frac{w}{n(n+nw)}x_\ell$
 - 15: **end parfor**
 - 16: Set $\mathbf{X}_{(i)}^\top = \left[(\mathbf{X}_{(i)}^{(1)})^\top \mid (\mathbf{X}_{(i)}^{(2)})^\top \mid \dots \mid (\mathbf{X}_{(i)}^{(m)})^\top \right]$
 - 17: Compute $\sigma(\mathbf{X}_{(i)})$ as in Remark 3
 - 18: **end while**
 - 19: Output the final iteration $\mathbf{X}_{(\text{final})}$
-

With the form of \mathbf{L}^\dagger computed above, we exploit the special structure of $B(\mathbf{X}_{(i-1)})$ to further speed up the calculation of $\mathbf{L}^\dagger B(\mathbf{X}_{(i-1)})\mathbf{X}_{(i-1)}$ needed in the i th iteration of the JOFC algorithm. We first note that $B(\mathbf{X}_{(i-1)})$ is block diagonal, with m diagonal blocks each of size $n \times n$. We will denote the diagonal blocks of $B(\mathbf{X}_{(i-1)})$ by B_1, B_2, \dots, B_m . By construction,

$$\mathbf{1}_{mn}^\top B(\mathbf{X}_{(i-1)}) = B(\mathbf{X}_{(i-1)})\mathbf{1}_{mn} = 0,$$

and therefore $\mathbf{1}_n^\top B_j = B_j\mathbf{1}_n = 0$ for all $j = 1, 2, \dots, m$. It follows that $B_j J_n = J_n B_j = 0$ for all $j = 1, 2, \dots, m$. Defining

$$A' := \frac{n+w}{n(n+mw)}I_n, \text{ and } B' := \frac{w}{n(n+mw)}I_n,$$

the resulting calculation of $\mathbf{L}^\dagger B(\mathbf{X}_{(i-1)})\mathbf{X}_{(i-1)}$ is computationally very simple:

$$\mathbf{L}^\dagger B(\mathbf{X}_{(i-1)})\mathbf{X}_{(i-1)} = \begin{bmatrix} A' & C' & C' & \cdots & C' \\ C' & A' & C' & \cdots & C' \\ C' & C' & A' & \cdots & C' \\ \vdots & \vdots & \vdots & \ddots & \vdots \\ C' & C' & C' & \cdots & A' \end{bmatrix} B(\mathbf{X}_{(i-1)})\mathbf{X}_{(i-1)}.$$

If we write $\mathbf{X}_{(i-1)}$ as

$$\mathbf{X}_{(i-1)}^\top = \left[(\mathbf{X}_{(i-1)}^{(1)})^\top | (\mathbf{X}_{(i-1)}^{(2)})^\top | \cdots | (\mathbf{X}_{(i-1)}^{(m)})^\top \right],$$

then

$$[B(\mathbf{X}_{(i-1)})\mathbf{X}_{(i-1)}]^\top = \left[(B_1\mathbf{X}_{(i-1)}^{(1)})^\top | (B_2\mathbf{X}_{(i-1)}^{(2)})^\top | \cdots | (B_m\mathbf{X}_{(i-1)}^{(m)})^\top \right].$$

Combined with a fast initialization, we get the Fast JOFC (fJOFC) algorithm, Algorithm 2.

Remark 6. Note that calculation of \mathbf{L}^\dagger in the JOFC algorithm has algorithmic complexity $O((mn)^3)$ given an SVD (or QR decomposition) based pseudoinverse algorithm. Additionally, each iteration has algorithmic complexity $O((mn)^2d)$. Therefore, given a bounded number of iterations and assuming $d < mn$, the JOFC algorithm has algorithmic complexity $O((mn)^3)$. In fJOFC, we algebraically compute \mathbf{L}^\dagger , and each iteration has algorithmic complexity $O(mn^2d)$ if run in serial, and $O(mn^2d/c)$ if run on c parallel processors. Therefore, given a bounded number of iterations, the fJOFC algorithm has algorithmic complexity $O(mn^2d)$ in serial and $O(mn^2d/c)$ if run on c parallel processors, showing the potential for the dramatically increased efficiency achievable with fJOFC.

3 Results

In this section we demonstrate the dramatic efficiency increase achievable by fJOFC versus JOFC over a variety of real and simulated data examples. In all examples, the algorithms were implemented on a MacBook Pro with a 2.6 GHz Intel Core i5 processor and 4GB 1600 MHz DDR3 memory.

3.1 Simulations

Let $Y \in \mathbb{R}^{400 \times 2}$ have rows which are independent 2-dimensional Gaussian $((5, 5), I_2)$ random variables. Letting $z = \max(Y) - \min(Y)$, for $i = 1, 2, \dots, 6$, we set Y_i to be $Y + E_i$, with the entries of

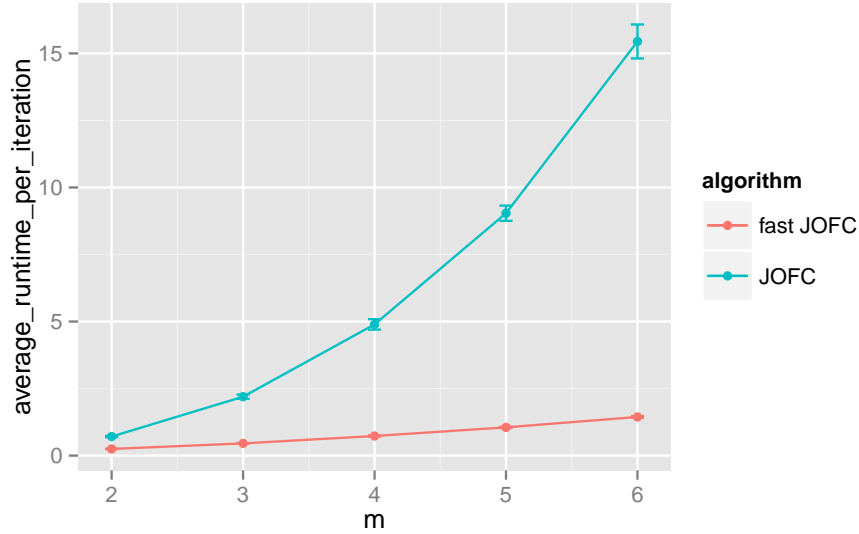


Figure 1: With $n = 400$, and $m = 2, 3, 4, 5, 6$, we embed $\Delta \in \mathbb{R}^{nm \times nm}$ via fJOFC and JOFC using identical initial configurations $\mathbf{X}_{(0)} = \text{cMDS}(\Delta^{(m)})$. We then plot the average run time per iteration ($\pm 2s.e.$) versus m for both JOFC and fJOFC, averaged over 50 Monte Carlo replicates.

E_i being independent $\text{Uniform}(-z/50, z/50)$ random variables, which are also independent across i , and we set Δ_i to be the interpoint distance matrix of Y_i . These $\{Y_i\}$ represent our $n = 400$ objects measured under $m = 6$ modalities. For $m = 2, 3, \dots, 6$, we embed into \mathbb{R}^2 (with η defined as in Section 2)

$$\Delta = \begin{bmatrix} \Delta_1 & \eta & \cdots & \eta \\ \eta & \Delta_2 & \cdots & \eta \\ \vdots & \vdots & \ddots & \vdots \\ \eta & \eta & \cdots & \Delta_m \end{bmatrix},$$

with both fJOFC (in serial) and JOFC using identical initial configurations $\mathbf{X}_{(0)} = \text{cMDS}(\Delta^{(m)})$, (classical MDS, see [25, 2]) and we plot the average run time per iteration versus m for both fJOFC and JOFC in Figure 1, averaged over 50 MC replicates. Even in this relatively small simulation, the increased runtime speed is dramatically illustrated in Figure 1 (even with fJOFC run in serial), with the ratio of the average run times (JOFC versus fJOFC) being (2.86, 4.82, 6.70, 8.59, 10.71) for $m = (2, 3, 4, 5, 6)$, suggesting that fJOFC is nearly a factor of m ($\approx 1.6m$) faster than JOFC here; contrast this with Remark 6.

We next consider the case of fixed $m = 3$ and varying $n = (200, 400, 600, 800, 1000)$. With Y and Δ defined as above, we again embed $\Delta \in \mathbb{R}^{nm \times nm}$ into \mathbb{R}^2 via fJOFC (in serial) and JOFC using identical initial configurations $\mathbf{X}_{(0)} = \text{cMDS}(\Delta^{(m)})$. In Figure 2, we plot the average run time per iteration versus n for both JOFC and fJOFC, averaged over 50 MC replicates. Again,

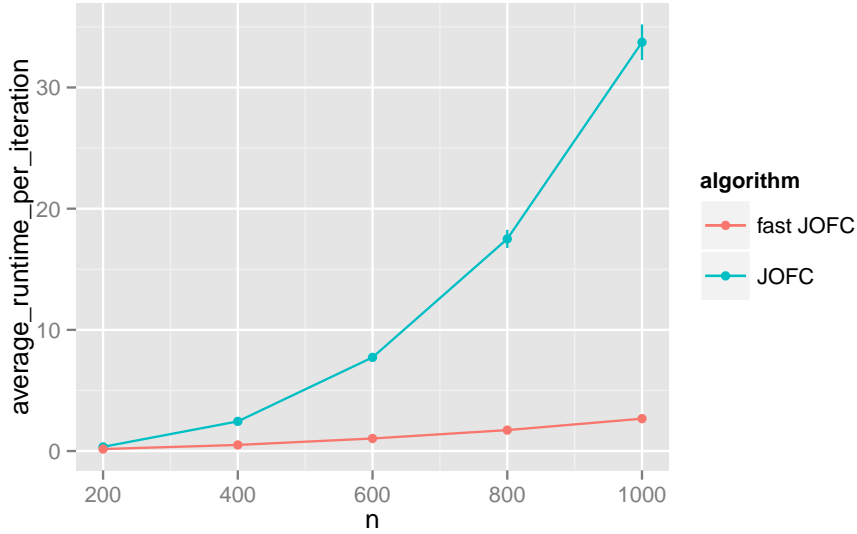


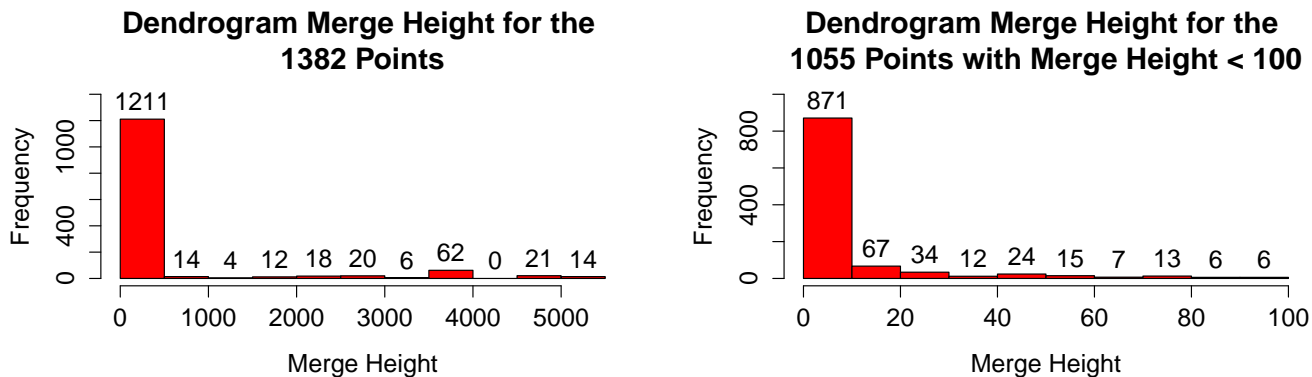
Figure 2: With $n = (200, 400, 600, 800, 1000)$ and $m = 3$, we embed $\Delta \in \mathbb{R}^{nm \times nm}$ via fJOFC and JOFC using identical initial configurations $\mathbf{X}_{(0)} = \text{cMDS}(\Delta^{(m)})$. We then plot the average run time per iteration ($\pm 2s.e.$) versus n for both JOFC and fJOFC, averaged over 50 Monte Carlo replicates.

note the dramatic speedup achieved by fJOFC, with the ratio of the average run times (JOFC versus fJOFC) being $(2.10, 4.86, 7.45, 10.13, 12.63)$ for $n = (200, 400, 600, 800, 1000)$, suggesting that fJOFC is nearly a factor of n ($\approx 0.12n$) faster than JOFC here, as suggested by Remark 6.

3.2 Wikipedia

We further demonstrate the utility of our algorithm on a multimodal Wikipedia data set. We collect the $n = 1382$ articles $\{y_{1i}\}_{i=1}^{1382}$ from English Wikipedia which compose the 2-hop neighborhood of the article entitled “Algebraic Geometry” (where articles are linked if there exists a hyperlink in one article to the other, and these links are considered undirected). There is a natural 1-1 correspondence between these articles and their versions in French Wikipedia, and we will denote the associated French articles by $\{y_{2i}\}_{i=1}^{1382}$. As in [23], each $\{y_{ji}\}_{i=1}^{1382}$ for $j = 1, 2$, further gives rise to two measures of inter-article dissimilarity: Δ_{j1} , the shortest path distance in the undirected hyperlink graph; and Δ_{j2} , the cosine dissimilarities between text feature vectors (provided by latent semantic indexing [7]) associated with each article. We use fJOFC (with $w = 10$) to embed these $n = 1382$ points across $m = 4$ modalities into \mathbb{R}^{10} . Note that implementing our fJOFC algorithm in serial ran in ≈ 42.2 minutes while the JOFC algorithm with the same settings ran in ≈ 10.37 hours (a factor of ≈ 14.7 speed-up).

In this omnibus embedding, if all 4 embedded versions of a single Wikipedia article lie close



(a) Dendrogram merge heights for all $n = 1382$ points. (b) Dendrogram merge heights for the $n = 1055$ points with merge height < 100 .

Figure 3: Histograms showing, for each of the $n = 1382$ points in (a) and for each of the $n = 1055$ points with merge height < 100 in (b), the height in the hierarchical clustering dendrogram when each of the four modalities was first merged into a single cluster for that point.

together, then this article’s relationship to all of the other articles is preserved across modality. To explore this, we hierarchically cluster (using Ward’s method [13]) the 5528 points and compute the pairwise cophenetic distance (the height in the resulting dendrogram at which the two points are first clustered together) between each of the points. If the dissimilarities are well preserved across modality, then the maximum cophenetic distance between two embedded versions of the same article (we call this the *Dendrogram Merge Height* or DMH) should be small.

In Figure 3(a), we plot a histogram of the DMH’s for the 1382 articles, and note that over 76% of the articles have DMH less than 100. In Figure 3(b) we see that over 63% of the articles have DMH less than 10. To further confirm that the dissimilarities are well preserved across modality, we calculated cluster labels given by the hierarchical clustering dendrogram at height $h \in [0, 2]$. We then compute the adjusted Rand index [12] (ARI) between these clusterings and the ground truth clustering (given by the 1382 size 4 clusters each composed of a single article across modalities), and plot this in Figure 4. From the figure, we see that the clustering is not only grossly clustering the article 4-tuples together, but is also capturing the fine-grain differences between the different articles as well.

If the ARI between the hierarchical clustering and the ground truth clustering was equal to 1, then the structure of the four dissimilarities would be nearly identical, and joint inference across modality would yield minimal gain over separately embedding the Δ_i ’s and then applying subsequent inference methodologies. From Figures 3(a)-3(b) and 4, we see this is not the case. Indeed, we see that for some articles the relative geometry in the four modality-specific embeddings

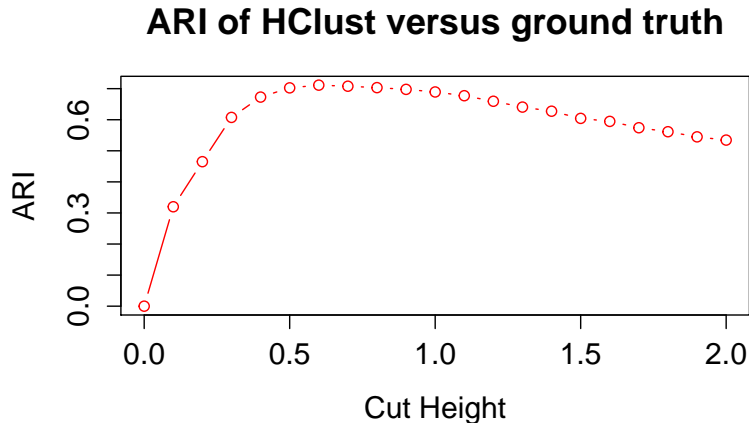


Figure 4: The adjusted Rand index between the clusters given by the hierarchical clustering dendrogram at height $h \in [0, 2]$ and the ground truth clustering (given by the 1382 size 4 clusters each composed of a single article across modalities).

is not commensurate. We illustrate this in Figure 5, where we plot a branch of the hierarchical clustering dendrogram when the tree is cut at height 20. Note that although the four modality-specific embeddings of many articles (article 454 is highlighted here in blue as an example) are very similar, some of the articles’ embeddings are not preserved well across modality (article 366 is highlighted here in red as an example; note that the English graph with shortest path distance differs significantly from the other three modalities for this article). These misclustered articles inform both how and why the modalities differ, and by studying these pathologies further, we hope to better understand the data features that are emphasized by graph-based versus text-feature-based methodologies.

Note that had we set $w \gg 10$, these misclusterings would have been corrected in the embedding and the embedding would not have been as informative about the different topologies in the different Δ_i ’s. Had we set $w \ll 10$, we would have been unable to identify articles across modality and the embedding would not be as informative about the matchedness of the different Δ_i ’s. This illustrates a key feature of the JOFC algorithm, as a well-chosen weighting w allows for the preservation of cross-modality matchedness while not forcing incommensurate versions of the data points to be artificially embedded close to one another.

4 Conclusion

The JOFC algorithm has proven to be a valuable and adaptable tool for a variety of inference tasks ((e.g., graph matching [17]; hypothesis testing [21]; joint classification [24]). The key capability

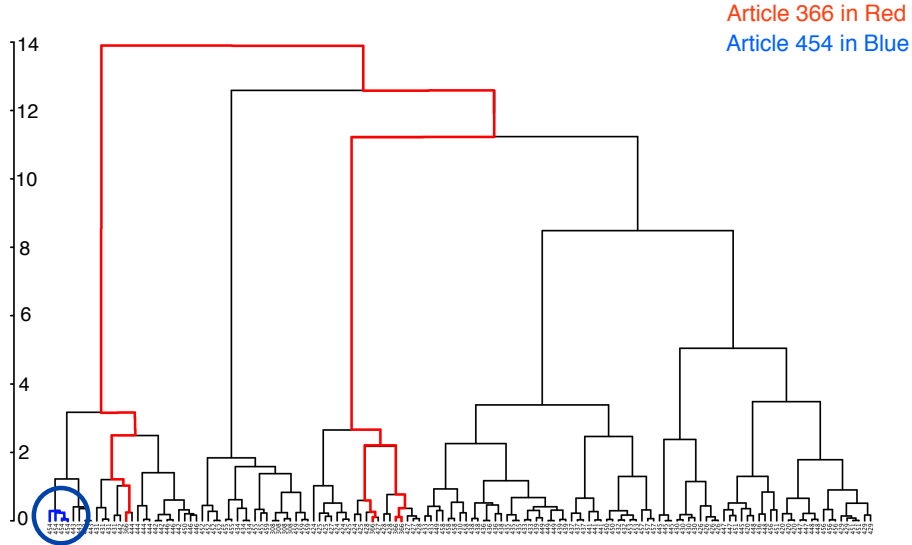


Figure 5: A branch of the hierarchical clustering dendrogram when the tree is cut at height 20. Note that the four modality-specific embeddings of article 454 (highlighted in blue in the dendrogram) are very similar, while those of article 366 are not (the English graph with shortest path distance differs significantly from the other three modalities for this point).

enabled by our fJOFC algorithm versus the JOFC algorithm is enhanced scalability in m and n ; indeed, for a fixed n , we see a factor of m speed-up over the JOFC algorithm, and for a fixed m we see a factor of n speed up achieved by fJOFC. Combined with sparse dissimilarity representations of very large data sets, this capability to simultaneously embed many different large dissimilarities enables the complex structure of the data to more easily be interrogated, leading to potentially significant discoveries heretofore beyond our grasp.

While the sequential Guttman transforms computed in Algorithm 1 are globally convergent to a set of local minimizers of $\sigma(\mathbf{X})$, in most cases, the local convergence rate of the iterative Guttman transforms is linear [4]. However, in practice the sequential Guttman transforms often exhibit good global properties, and only a few iterations are required to obtain a sufficiently good suboptimal embedding [15]. Analyzing these global properties and/or modifying fJOFC to accelerate the linear convergence (for example, by adding a step-size procedure into the successive Guttman transforms as in [5, 6], or by applying Newton’s method to optimize $\sigma(\mathbf{X})$ as in [15]) are essential next steps for further scaling fJOFC to very big data.

References

- [1] S. Adali and C. E. Priebe. Fidelity-commensurability tradeoff in joint embedding of disparate dissimilarities. *arXiv preprint, arXiv:1306.1977*, 2013.
- [2] I. Borg and P. J. F. Groenen. *Modern Multidimensional Scaling: Theory and Applications*. Springer, 2005.
- [3] J. de Leeuw. Applications of convex analysis to multidimensional scaling. In *Recent Developments in Statistics (Proc. European Meeting Statisticians, Grenoble, 1976)*, pages 133–145. North-Holland, Amsterdam, 1977.
- [4] J. de Leeuw. Convergence of the majorization method for multidimensional scaling. *Journal of Classification*, 5(2):163–180, 1988.
- [5] J. De Leeuw and W. J. Heiser. Multidimensional scaling with restrictions on the configuration. *Multivariate Analysis*, 5:501–522, 1980.
- [6] J. De Leeuw and I. Stoop. Upper bounds for kruskal’s stress. *Psychometrika*, 49(3):391–402, 1984.
- [7] S. C. Deerwester, S. T. Dumais, T. K. Landauer, G. W. Furnas, and R. A. Harshman. Indexing by latent semantic analysis. *JASIS*, 41(6):391–407, 1990.
- [8] A. Elgammal and C.-S. Lee. Inferring 3d body pose from silhouettes using activity manifold learning. In *Proceedings of the 2004 IEEE Computer Society Conference on Computer Vision and Pattern Recognition, 2004*, volume 2, pages II–681. IEEE, 2004.
- [9] J. C. Gower. An application of the modified Leverrier–Faddeev algorithm to the spectral decomposition of symmetric block-circulant matrices. *Computational Statistics and Data Analysis*, 50(1):89–106, 2006.
- [10] J. C. Gower and P. J. F. Groenen. Applications of the modified Leverrier-Faddeev algorithm for the construction of explicit matrix spectral decompositions and inverses. Technical report, University of Leiden, 1990.
- [11] D. Hardoon, S. Szedmak, and J. S. Shawe-Taylor. Canonical correlation analysis: An overview with application to learning methods. *Neural Computation*, 16(12):2639–2664, 2004.
- [12] L. Hubert and P. Arabie. Comparing partitions. *Journal of Classification*, 2(1):193–218, 1985.

- [13] S. C. Johnson. Hierarchical clustering schemes. *Psychometrika*, 32(3):241–254, 1967.
- [14] D. Karakos, J. Eisner, S. Khudanpur, and C. E. Priebe. Cross-instance tuning of unsupervised document clustering algorithms. In *HLT-NAACL*, pages 252–259. Citeseer, 2007.
- [15] A. J. Kearsley, R. A. Tapia, and M. W. Trosset. The solution of the metric STRESS and SSTRESS problems in multidimensional scaling using Newton’s method. Technical report, DTIC Document, 1995.
- [16] S. Lafon, Y. Keller, and R. R. Coifman. Data fusion and multicue data matching by diffusion maps. *Pattern Analysis and Machine Intelligence, IEEE Transactions on*, 28(11):1784–1797, 2006.
- [17] V. Lyzinski, S. Adali, J. T. Vogelstein, and C.E. Priebe. Seeded graph matching via joint optimization of fidelity and commensurability. *arXiv preprint, arXiv:1401.3813*, 2013.
- [18] Z. Ma, D. J. Marchette, and C. E. Priebe. Fusion and inference from multiple data sources in a commensurate space. *Statistical Analysis and Data Mining*, 5(3):187–193, 2012.
- [19] C. Nastar, B. Moghaddam, and A. Pentland. Generalized image matching: Statistical learning of physically-based deformations. In *Computer Vision ECCV’96*, pages 589–598. Springer, 1996.
- [20] S. J. Pan and Q. Yang. A survey on transfer learning. *Knowledge and Data Engineering, IEEE Transactions on*, 22(10):1345–1359, 2010.
- [21] C.E. Priebe, D.J. Marchette, Z. Ma, and S. Adali. Manifold matching: joint optimization of fidelity and commensurability. *Brazilian Journal of Probability and Statistics*, 27(3):377400, 2013.
- [22] M. Sahami and T. D. Heilman. A web-based kernel function for measuring the similarity of short text snippets. In *Proceedings of the 15th International Conference on the World Wide Web*, pages 377–386. ACM, 2006.
- [23] C. Shen and C. E. Priebe. Manifold matching using shortest-path distance and joint neighborhood selection. *arXiv preprint, arXiv:1412.4098*, 2014.
- [24] M. Sun and C. E. Priebe. Efficiency investigation of manifold matching for text document classification. *Pattern Recognition Letters*, 34(11):1263–1269, 2013.

- [25] W. S. Torgerson. Multidimensional scaling: I. Theory and method. *Psychometrika*, 17(4):401–419, 1952.
- [26] A. Vinokourov, N. Cristianini, and J. S. Shawe-Taylor. Inferring a semantic representation of text via cross-language correlation analysis. In *Advances in Neural Information Processing Systems*, pages 1473–1480, 2002.
- [27] C. Wang and S. Mahadevan. Manifold alignment using procrustes analysis. In *Proceedings of the 25th International Conference on Machine Learning*, pages 1120–1127. ACM, 2008.
- [28] C. Wang and S. Mahadevan. Manifold alignment without correspondence. In *IJCAI*, volume 2, page 3, 2009.
- [29] L. Wang and D. Suter. Learning and matching of dynamic shape manifolds for human action recognition. *Image Processing, IEEE Transactions on*, 16(6):1646–1661, 2007.

A Proof that \mathbf{L}^\dagger has the desired block matrix form

First note that

$$\mathbf{L} + \frac{1}{mn}J_{mn} = \begin{bmatrix} \alpha & \beta & \cdots & \beta \\ \beta & \alpha & \cdots & \beta \\ \vdots & \vdots & \ddots & \vdots \\ \beta & \beta & \cdots & \alpha \end{bmatrix} \quad (3)$$

is a block matrix with

$$\alpha = [n + w(m - 1)]I_n + \left(\frac{1}{mn} - 1\right)J_n, \quad \beta = -wI_n + \frac{1}{mn}J_n.$$

We will next find α' and β' such that

$$\left(\mathbf{L} + \frac{1}{mn}J_{mn}\right)^{-1} = \begin{bmatrix} \alpha' & \beta' & \cdots & \beta' \\ \beta' & \alpha' & \cdots & \beta' \\ \vdots & \vdots & \ddots & \vdots \\ \beta' & \beta' & \cdots & \alpha' \end{bmatrix} \quad (4)$$

where α' and β' are of the form

$$\alpha' = c_1 I_n + c_2 J_n, \quad \beta' = c_3 I_n + c_4 J_n.$$

Multiplying (3) and (4) yields a block matrix with (supressing subscripts)

$$\begin{aligned} c_1[n + w(m-1)]I + c_1 \left(\frac{1}{mn} - 1 \right) J + c_2[n + w(m-1)]J + c_2 n \left(\frac{1}{mn} - 1 \right) J \\ - c_3(m-1)wI + c_3 \frac{m-1}{mn} J - c_4(m-1)wJ + c_4 \frac{m-1}{m} J \end{aligned} \quad (5)$$

in its diagonal blocks, and

$$\begin{aligned} -c_1 wI + c_1 \frac{1}{mn} J - c_2 wJ + c_2 \frac{1}{m} J + c_3[n + w(m-1)]I + c_3 \left(\frac{1}{mn} - 1 \right) J + c_4[n + w(m-1)]J \\ + c_4 n \left(\frac{1}{mn} - 1 \right) J - c_3(m-2)wI + c_3 \frac{m-2}{mn} J - c_4(m-2)wJ + c_4 \frac{m-2}{m} J \end{aligned} \quad (6)$$

in its off-diagonal blocks. Now, setting (5) equal to I yields the following.

$$\begin{bmatrix} n + w(m-1) & -w(m-1) \\ -w & n + w \end{bmatrix} \begin{bmatrix} c_1 \\ c_3 \end{bmatrix} = \begin{bmatrix} 1 \\ 0 \end{bmatrix}$$

which yields

$$\begin{bmatrix} c_1 \\ c_3 \end{bmatrix} = \begin{bmatrix} \frac{n+w}{n(n+wm)} & \frac{w(m-1)}{n(n+wm)} \\ \frac{w}{n(n+wm)} & \frac{n+w(m-1)}{n(n+wm)} \end{bmatrix} \begin{bmatrix} 1 \\ 0 \end{bmatrix}.$$

Next, setting (6) equal to 0 yields

$$\begin{bmatrix} w(m-1) + \frac{1}{m} & -w(m-1) + \frac{m-1}{m} \\ -w + \frac{1}{m} & w + 1 - \frac{1}{m} \end{bmatrix} \begin{bmatrix} c_2 \\ c_4 \end{bmatrix} = \begin{bmatrix} \frac{-n+mn^2+mnw-wm}{n^2m(n+wm)} \\ \frac{-n+mnw-wm}{n^2m(n+wm)} \end{bmatrix},$$

giving that

$$\begin{bmatrix} c_2 \\ c_4 \end{bmatrix} = \begin{bmatrix} \frac{wm+m-1}{wm^2} & \frac{wm^2-wm-m+1}{wm^2} \\ \frac{wm-1}{wm^2} & \frac{wm^2-wm+1}{wm^2} \end{bmatrix} \begin{bmatrix} \frac{-n+mn^2+mnw-wm}{n^2m(n+wm)} \\ \frac{-n+mnw-wm}{n^2m(n+wm)} \end{bmatrix}.$$

This gives that

$$c_2 = \left(\frac{wm + m - 1}{wm^2} \right) \left(\frac{-n + mn^2 + mnw - wm}{n^2m(n + wm)} \right) + \left(\frac{wm^2 - wm - m + 1}{wm^2} \right) \left(\frac{-n + mnw - wm}{n^2m(n + wm)} \right)$$

$$= \frac{m^3nw^2 - m^3w^2 + m^2n^2w + m^2n^2 - m^2nw - mn^2}{wn^2m^3(n + wm)},$$

and

$$c_4 = \left(\frac{wm - 1}{wm^2} \right) \left(\frac{-n + mn^2 + mnw - wm}{n^2m(n + wm)} \right) + \left(\frac{wm^2 - wm + 1}{wm^2} \right) \left(\frac{-n + mnw - wm}{n^2m(n + wm)} \right)$$

$$= \frac{m^3nw^2 - m^3w^2 + m^2n^2w - m^2nw - mn^2}{wn^2m^3(n + wm)}.$$

The desired block form of \mathbf{L}^\dagger follows from

$$\mathbf{L}^\dagger = (\mathbf{L} + \frac{1}{mn} J_{mn})^{-1} - \frac{1}{mn} J_{mn}.$$